



Research

Study on Parameters of Modified Mohr–Coulomb Model for Water-rich Soft Soil in Tianjin, China



Huanfa Ma¹ · Xin Hao² · Yongpeng Yang² · Hui Li¹ · Lixin Yi²

Received: 16 March 2023 / Accepted: 7 June 2023

Published online: 15 June 2023

© The Author(s) 2023 [OPEN](#)

Abstract

Foundation pit excavation through the soft layer has great technical challenges and potential safety risks, especially in soft soil area. In this study, we use a 3D numerical model of Foundation pit to simulate the excavation process. Based on the simulation, the sensitivity analysis of the three stiffness parameters (E_{ur}^{ref} , E_{50}^{ref} and E_{oed}^{ref}) of the Modified Mohr–Coulomb model was carried out by using the Latin hypercube-one factor at a time method. During the simulation, the three stiffness parameters are changed with the perturbation amplitude of ($\pm 20\%$) and ($\pm 40\%$). In addition, the sensitivity of three stiffness parameters was calculated by taking the horizontal displacement of diaphragm wall as the observation index. Furthermore, by comparing the results of simulation with the measured data, the stiffness ratio relationship suitable for foundation pit simulation in Tianjin water-rich soft soil area are obtained. Our findings present that E_{ur}^{ref} is the parameter that has the largest influence on the uncertainty in the MMC model, while E_{oed}^{ref} is the least sensitive to horizontal displacement of diaphragm wall. The proportion rates of $E_{oed}^{ref}/E_{50}^{ref}$ and $E_{ur}^{ref}/E_{50}^{ref}$ provide a promising reference for simulating the foundation pit excavation in Tianjin water-rich soft soil area.

Article Highlights

1. MMC model can be used for numerical simulation of deformation characteristics of water-rich soft soil.
2. The applicability of LH-OAT method in the sensitivity analysis of MMC numerical simulation is verified.
3. The mechanical parameters of water-rich soft soil in the study area are suggested.

Keywords Modified Mohr–Coulomb Model (MMC model) · Water-rich soft soil · Latin Hypercube One factor at a Time (LH-OAT) method · Sensitivity analysis

1 Introduction

Soft soil generally refers to the soft-fluid-plastic clay with several engineering characteristics, such as high water content, large void ratio, high compressibility and low

shear strength. The soft soil in China is widely distributed and is mainly located in coastal, plain, inland lake basin, depression and river banks. The soft soil in coastal and plain areas is mostly located in the river downstream into the sea delta or alluvial plain, such as the Pearl River Delta

✉ Lixin Yi, yilixin@nankai.edu.cn; Huanfa Ma, zy20226633@163.com; Xin Hao, sanjin2850@163.com; Yongpeng Yang, yang_yongpeng@mail.nankai.edu.cn; Hui Li, zy2022016622@163.com | ¹China Communications Construction Company Tunnel Engineering Bureau Co. Ltd, Beijing 100024, China. ²College of Environmental Science and Engineering, Nankai University, Tianjin 300350, China.



SN Applied Sciences

(2023) 5:187

| <https://doi.org/10.1007/s42452-023-05411-x>

SN Applied Sciences
A **SPRINGER NATURE** journal

[1, 2], Tanggu and Minjiang estuary plain [3]. The inland lake basins and depressions are represented by Dongting Lake, Hongze Lake, Jiuhu Lake and Dianchi Lake [4, 5]. In engineering, soft soil is often subdivided into soft clay soil, silty soil, silt, peat soil and peat soil [6].

In recent years, great attention has been paid to stability problems associated with deep foundation pit excavation because of the continuous development of urban rail transit construction. Construction projects are often affected by external factors, such as site conditions during construction and tight construction schedule, etc. In the process of pursuing foundation pit excavation, mechanical properties of soft soil foundation and other conditions are easy to be ignored by the builders, which often becomes the pain point and difficulty in engineering construction. Under such conditions, the detection and protection of the whole excavation process must be strengthened in the excavation process, and thus minimize the risks causing heave of the pit bottom and even the collapse of the foundation pit [7].

Numerical simulation is an effective method to simulate the process of foundation pit excavation [8–10]. The constitutive models commonly used in numerical simulation are linear elastic model, Duncan–Chang (DC) model, Mohr–Coulomb (MC) model (including MMC model), Drucker–Prager (DP) model [11–15]. DC model is a nonlinear elastic model, which mainly describes the nonlinear characteristics of stress–strain relationship of soil mass. This model cannot reflect the dilatancy, softening and anisotropy of soil under shear, so it has some limitations. M–C model can reflect the strength of soil, which is more widely used in the simulation of geotechnical slope stability and tunnel excavation [16, 17]. However, the influence of unloading on soil deformation modulus is not considered in the model, which leads to large uplift deformation during foundation pit excavation, so it is not suitable for the simulation of foundation pit excavation. Although the Drucker–Prager model is easy to program, it's not appropriate to describe the actual behavior of earth. The defects of the MC model also apply to the DP mode. Considering the stress dependence of soil stiffness, the MMC model can simulate soil deformation under different stress paths and stress histories under loading and unloading.

In our study site in Tianjin, the soil is soft soil and its geological environment is fragile. Based on the MMC model setup for Tianjin, this paper simulates the excavation process of a transfer station of the Tianjin city subway lines 11 (under construction) and line 6. Compared with the MC model, the MMC model introduces three stiffness parameters: reference secant modulus (E_{50}^{ref}), reference tangent modulus ($E_{\text{oad}}^{\text{ref}}$) and unloading and reloading modulus ($E_{\text{ur}}^{\text{ref}}$), which solves the unreasonable loading

and unloading problems of the MC model. Therefore, the MMC model is more suitable for the numerical simulation of foundation pit excavation. The determination of the stiffness parameters ($E_{\text{ur}}^{\text{ref}}$, E_{50}^{ref} and $E_{\text{oad}}^{\text{ref}}$) is more difficult to obtain than that of other strength parameters. For example, the stiffness parameters of the soil will change with the change of the stress state of the soil, and the stiffness parameters obtained by different stress paths will also be different. The study of Brinkgreve [18] showed that the undrained Young's modulus was three times higher than the shear modulus, while the drained Young's modulus was 1.5–2 times lower than the shear modulus, indicating that the stiffness parameters differed greatly under different conditions. Therefore, the sensitivity study of stiffness parameter plays an important role in the study of foundation pit deformation in soft soil area.

There are two methods to select the soil model parameters. One is to take the undisturbed soil for laboratory test and analyze the model parameters according to the test results [19–22]. However, the process of collecting and preparing soil samples may have an impact on the soil. The other method is based on the measured data and numerical calculation for parameter inversion, the main idea is that by changing the soil parameters, the calculated results are constantly close to the measured results, so as to obtain the soil mechanical parameters [23–25].

In order to quantitatively judge the influence of these three parameters on the model results and determine the value most in line with the actual field situation, sensitivity analysis was conducted on $E_{\text{ur}}^{\text{ref}}$, E_{50}^{ref} and $E_{\text{oad}}^{\text{ref}}$ respectively. Sensitivity analysis can not only reduce the computational cost of further uncertainty analysis, but also help restoring the real environmental conditions to the greatest extent, providing a theoretical basis for risk analysis and model calibration in subsequent engineering construction. Therefore, the objective of this study is to determine the optimal value of $E_{\text{ur}}^{\text{ref}}$, E_{50}^{ref} and $E_{\text{oad}}^{\text{ref}}$ in the MMC model for foundation pit excavation by applying the sensitivity analysis using the Latin Hypercube One Factor (LH-OAT) method and comparing the monitoring data with the numerical simulation results. In the next section, we introduce the general situation of the research area and the research methods. Section 3 shows the relation between the three parameters and the horizontal displacement of the ground diaphragm wall. In Sect. 4, we present the relationships between stiffness parameters in different regions. Finally, Sect. 5 present conclusions drawn from the study. The results from this study will also provide theoretical support for foundation pit excavation in water-rich soft soil area.

2 Materials and methods

2.1 Overview and study area

The Mohr–Coulomb model (MC) is an ideal elastic–plastic model, its linear criterion may be expressed as follow [* MERGEFORMAT 26]:

$$\frac{\sigma_1 - \sigma_3}{2} = c \cos \varphi + \frac{\sigma_1 + \sigma_3}{2} \sin \varphi \tag{1}$$

where σ_1 and σ_3 is the major and minor principal stress components, respectively; φ is the frictional angle.

In Eq. (1), the elastic modulus is adopted in the process of excavation and unloading. However, the stress–strain relationship before failure is linear elastic, so the nonlinear deformation behavior of soil cannot be well described, and the influence of stress path on the mechanical properties of soil cannot be considered [27].

The modified Mohr–Coulomb model (MMC) combines the nonlinear elastic model with the elastic–plastic model

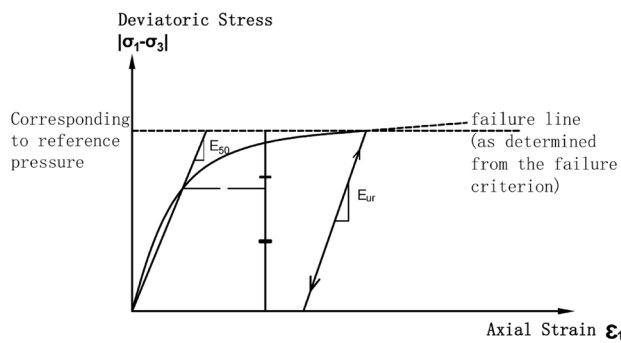


Fig. 1 Hyperbolic stress–strain relationship of conventional triaxial drainage test, where E_{50} is secant Young’s modulus at 50% of the ultimate deviatoric stress, E_{ur} is unloading–reloading secant Young’s modulus

to establish the double yield surface elastic–plastic model. This model assumes that the axial strain ϵ_1 and the deflection stress q of the triaxial drainage loading test behaves as hyperbola pattern (Fig. 1). Based on the Mohr–Coulomb failure criterion, E_{ur}^{ref} , E_{50}^{ref} and E_{oed}^{ref} were used to describe the soil strength, which solved the unreasonable loading and unloading problem of the Mohr–Coulomb model (Table 1).

The stress–strain relationship of MMC model during elastic deformation is shown as follows [28–30]:

$$\epsilon_1 = \frac{2 - R_f}{2E_{50}} \frac{q}{1 - q/q_a} \tag{2}$$

$$E_{50} = E_{50}^{ref} \left(\frac{\sigma_3 + \cot^{-1} \varphi}{\sigma^{ref} + \cot^{-1} \varphi} \right)^m \tag{3}$$

$$q_a = \frac{q_f}{R_f} \tag{4}$$

At the stage of plastic deformation, the shear yield function F_s is described by the following equations:

$$F_s = \frac{q_a}{E_{50}} \frac{q}{q_a - q} - \frac{2q}{E_{ur}} - \gamma_p = 0 \tag{5}$$

$$\gamma_p = \epsilon_1^p - \epsilon_2^p - \epsilon_3^p \approx 2\epsilon_1^p \tag{6}$$

$$E_{ur} = E_{ur}^{ref} \left(\frac{\sigma_3 + \cot^{-1} \varphi}{\sigma^{ref} + \cot^{-1} \varphi} \right)^m \tag{7}$$

The non-associated plastic flow rule is derived from the following plastic potential function:

$$Q_s = \frac{\sigma_1 - \sigma_3}{2} - \frac{\sigma_1 + \sigma_3}{2} \sin \psi_m \tag{8}$$

Table 1 Parameters of the Mohr–Coulomb model

Symbols	Name	Methods or standard value
c	Cohesion	Triaxial compression test
φ	Frictional Angle	Triaxial compression test
ψ	Friction Angle at shear	
n	Porosity	Laboratory test
E_{50}^{ref}	Secant Elastic Modulus in Shear Hardening	Triaxial compression test
E_{oed}^{ref}	Tangential Stiffness Primary Oedometer Test Loading	One-dimensional compression test
E_{ur}^{ref}	Elastic Modulus at Unloading	Triaxial compression test
m	Power of Stress Level Dependency	0.5 ~ 1.0 Clay: 0.7 ~ 0.9
K_0	Coefficient of Static Earth Pressure	$K_0 = 1 - \sin \varphi$
R_f	Failure Ratio	0.9
σ^{ref}	Reference Pressure	100 kPa

Compression yield function F_v is expressed in the following form:

$$F_v = \frac{\tilde{q}^2}{M^2} + p^2 - p_0^2 \tag{9}$$

The plastic potential function of the compressed yield surface which adopts the associated flow rule is given by:

$$Q_v = \frac{\tilde{q}^2}{M^2} + p^2 \tag{10}$$

where q_f is the ultimate deviatoric stress; q_a is the asymptotic deviatoric stress; $\epsilon_1^p, \epsilon_2^p, \epsilon_3^p$ are the plastic strains in three principal stress directions; p is the mean effective pressure; p_0 is the pre-consolidation pressure; \tilde{q} is Roscoe's invariant of deviatoric part of the stress tensor. Other parameters of the model are shown in the following table:

2.2 LH-OAT

Common sampling methods include Monte Carlo method, First-order quadratic matrix analysis method, etc. Monte Carlo method is relatively simple and easy to operate, but it requires a lot of calculation. The first-order quadratic matrix analysis method cannot be used for highly nonlinear functions and error analysis. Latin hypercube sampling (LHS) improves the calculation accuracy and efficiency by reducing the variance. Sensitivity analysis can be divided into local Sensitivity analysis methods and global Sensitivity analysis methods, such as Morris, Sobol', Fourier Amplitude Sensitivity Test, etc. Morris could not calculate sensitivity quantitatively, and Sobol's calculation cost was high [32]. Fourier Amplitude Sensitivity Test cannot obtain the Sensitivity of the interaction between parameters [33]. The OAT (One-factor-At-a-Time) method, which changes one input

factor at a time while keeping the others fixed between two successive model evaluations, is a global sensitivity analysis method. It has low computational cost and simple calculation. This paper applies LH-OAT method for subsequent research.

The LHS method divides the distribution of each parameter into N and guarantees equal-probability sampling. Its computation is effective [34]. However, the sensitivity analysis of one specific parameter can't be obtained by this strategy [35]. The LH-OAT sensitivity analysis method combines OAT design and the LH sampling by taking the LH sampling as initial points for an OAT design [36]. In this study, the sensitivity, S , for each parameter, x_j , is then calculated as [37]:

$$S = \frac{|f(x_1, x_2, x_3, \dots, x_j(1 + \Delta_j)) - f(x_1, x_2, x_3, \dots, x_j)_{min}|}{f(x_1, x_2, x_3, \dots, x_j)_{min}} \tag{11}$$

$$\bar{S} = \frac{1}{n} \sum_{i=1}^n S \tag{12}$$

where $f()$ refers to the model function, $f()_{min}$ is the minimum value of the function, Δ_j is the fraction by which the parameter is changed, j refers to a LH point, each LH sample point is varied for i times.

2.3 Study area

Tianjin city, located in the north part of The North China Plain, west of the Bohai Sea, is a typical soft soil area in China. Its strata have obvious characteristics of sea and land cross deposition. The soft soil layer of Tianjin plain was mainly formed in the Huanghua Transgression period of 8000–2500 years ago. At the same time, because Tianjin is located in the low-lying center of Tianjin plain and

Table 2 Strata and their physical and mechanical properties [40]

Strata Serial	Name of Soil Layer	Spt blow count	Bulk Density $\gamma/(KN/m^3)$	$c/(kPa)$	$\varphi/(^\circ)$	$\psi/(^\circ)$	$\sigma^{ref}/(KPa)$	n	R_f	K_0	m	Water content $w/(%)$
1–1	Mixed fill layer	4	19.5	18	13	0	100	0.61	0.9	0.78	0.5	30.9
4–1	Silt clay	5	19.4	12.4	16.4	0	100	0.81	0.9	0.72	0.6	31.4
6–3	Clay silt	13.5	19.4	8.1	24.5	0	100	0.75	0.9	0.59	0.7	27.1
6–4	Silty clay	7.3	18.5	12	15.2	0	100	0.85	0.9	0.74	0.6	29.8
7–1	Silty clay	7	19.7	11.3	16.1	0	100	0.77	0.9	0.72	0.6	27.3
8–2	Sandy silt	28	19.9	9.9	24.1	0	100	0.61	0.9	0.59	0.7	19.5
9–1	Clay silt	13	19.7	13.1	17.3	0	100	0.63	0.9	0.70	0.6	24.9
10–1	Clay	14.5	20.7	12.2	17.7	0	100	0.73	0.9	0.70	0.8	25.6
11–1	Silty clay	17	20.3	16.5	17.6	0	100	0.67	0.9	0.70	0.6	23.6
12–1	Silty clay	20.5	20.3	20.7	18.8	0	100	0.74	0.9	0.68	0.6	26.4

was affected by diversion of the ancient Yellow River three times, the southern Plain of Tianjin is mainly composed of alluvium, lacustrine and Marine deposits. The northern and central parts are dominated by continental impulse and impulse deposits [3, 38, 39].

According to the existing geotechnical investigation, the foundation soils of our study site, the transfer station of the Tianjin city subway line 11 (under construction) and line 6 are all Quaternary unconsolidated sediments. The whole formation consists of three marine strata (6, 10, 12) and five continental strata (4, 7, 8, 9, 11) which are refined into 10 layers according to their physical and mechanical properties, as shown in Table 2. The soft soil in the study area has a high water content, ranging from 19.5% to 31.4%, with an average water content of 26.65%.

2.4 Sensitivity calculation scheme

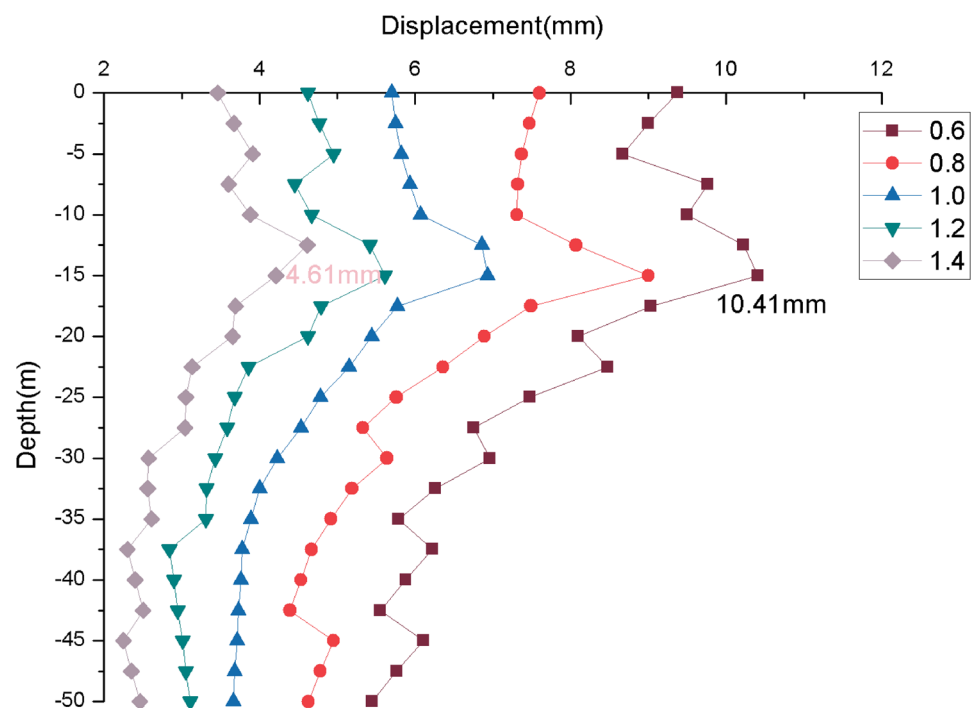
Numerical simulation method was applied to establish a model for the deep foundation pit. The model was established according to the actual engineering size, with x direction of 350 m, y direction of 380 m and Z direction of 60 m. During the modeling process, solid elements were used for soil, beam elements were used for the bracing structures, and plate elements were used for ground wall. The simulation process is consistent with the actual construction steps. According to the design, the foundation pit and the bracing structure are established in five steps, each step includes soil excavation and bracing structure construction. The depth of the first excavation was 7.2 m.

The excavation depths of the other four stages are 6.2 m, 5.4 m, 5.6 m and 2.8 m, respectively. The bracing structures are located at depths of 0 m, 7.2 m, 13.4 m, 23.2 m and 26 m respectively.

In the calculation, the structural stress is ignored, the initial stress field is assumed to be the gravity stress field, and the soil is regarded as an elastic–plastic continuum, which is simulated by the MMC model. Since the horizontal displacement of diaphragm wall is an important index to measure the deformation of foundation pit and is also a common index for monitoring the construction process of foundation pit, this research selects the horizontal displacement of diaphragm wall as parameter evaluation index.

In order to understand the influence of three stiffness parameters on the horizontal displacement of diaphragm wall during simulation, LH-OAT method was used to analyze the influence of E_{ur}^{ref} , E_{50}^{ref} and E_{oed}^{ref} on diaphragm wall of different soil layers (Table 2). The LH method divides the distribution of each parameter into 5 strata with a probability of occurrence equal to $\frac{1}{5}$. According to the OAT method, changing the value of only one factor while keeping the others fixed, the perturbation amplitude of three stiffness parameters is ($\pm 20\%$) and ($\pm 40\%$). The sensitivity of each soil layer under the disturbance of different parameters can be obtained by Formula (11), and the mean value of sensitivity calculation results is calculated by using Formula (12). Based on the sensitivity calculation results, the horizontal displacement of diaphragm wall in different soil layers is compared with the monitoring data,

Fig. 2 Horizontal displacement curves of the diaphragm wall caused by E_{ur}^{ref}



so as to obtain the optimal parameters for soft soil layer modeling in Tianjin.

3 Results

3.1 Correlation analysis for E_{ur}^{ref} , E_{50}^{ref} and E_{oed}^{ref}

In the same soil layer, two parameters are fixed and the

Fig. 3 Horizontal displacement curves of the diaphragm wall caused by E_{50}^{ref}

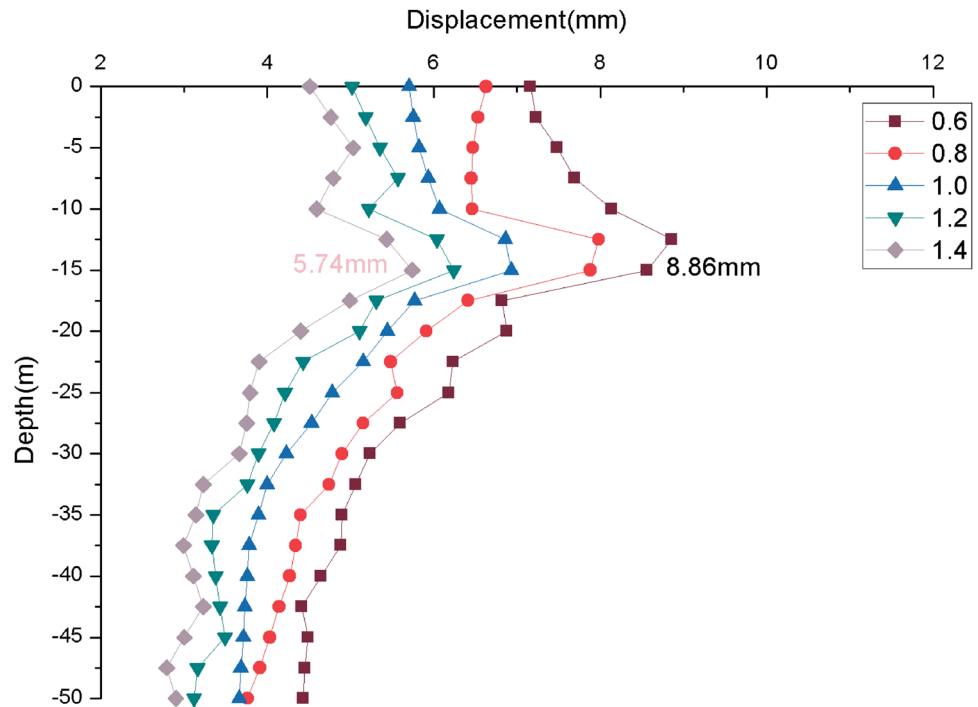
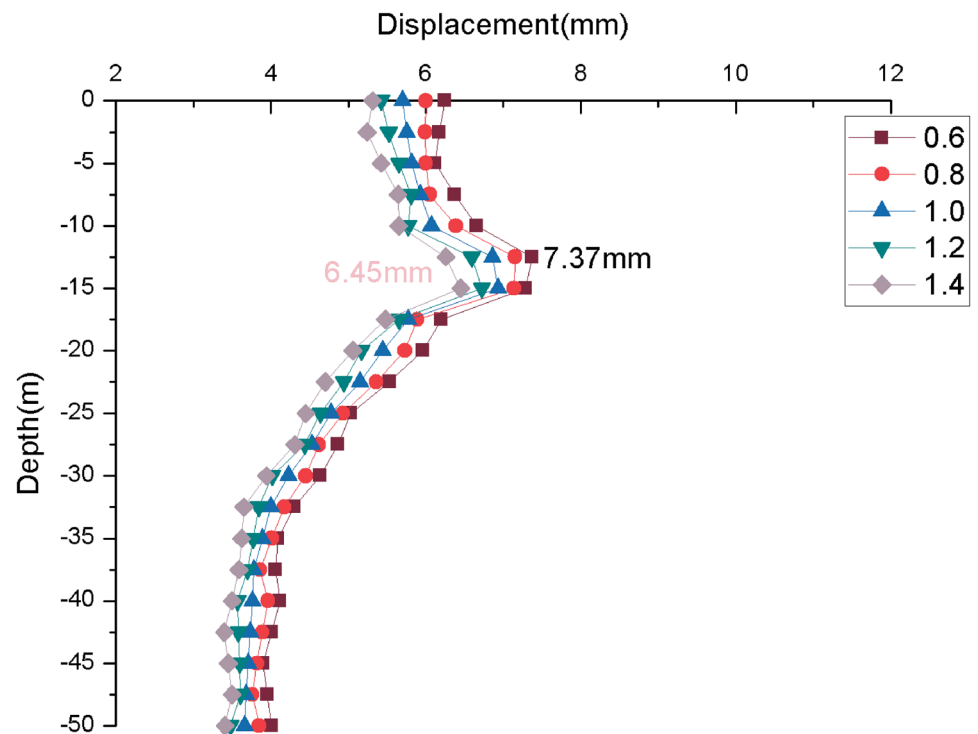


Fig. 4 Horizontal displacement curves of the diaphragm wall caused by E_{oed}^{ref}



other parameter is disturbed by ($\pm 20\%$) and ($\pm 40\%$) to calculate the horizontal displacement of diaphragm wall caused by changes in E_{ur}^{ref} , E_{50}^{ref} and E_{oed}^{ref} . Figure 2–4 gives the horizontal displacement curves of three parameters at different depth. Figure 2 shows the horizontal displacement of the diaphragm wall caused by (-40%) of the disturbance of E_{ur}^{ref} having maximum deformation of 10.41 mm and maximum deformation of 4.61 mm caused by 40% of the disturbance. The difference is 5.80 mm. Figure 3 shows the horizontal displacement of the diaphragm wall caused by ($\pm 40\%$) of the disturbance of E_{50}^{ref} having a maximum value of deformation equal to 8.86 mm and 5.74 mm. Figure 4 shows the horizontal displacement of the diaphragm wall caused by ($\pm 40\%$) of the disturbance of E_{oed}^{ref} having a maximum value of deformation equal to 7.37 mm and 6.45 mm. The corresponding difference of E_{50}^{ref} and E_{oed}^{ref} are 3.12 mm and 0.92 mm, respectively. It can be seen that the absolute values of horizontal displacement were highest when disturbances of parameters are (-40%). The influence of parameters in the same soil layer is ranked as $E_{ur}^{ref} > E_{50}^{ref} > E_{oed}^{ref}$ and parameters are negatively correlated with the horizontal displacement.

3.2 Sensitivity analysis for E_{ur}^{ref} , E_{50}^{ref} and E_{oed}^{ref}

A sensitivity analysis for the three parameters by the LH-OAT method is conducted in 10 soil layers. The correlation

sensitivity of the variation of the diaphragm wall in different soil layers is compared. It can be seen from the calculation results (demonstrated in Fig. 5) of the model that the horizontal displacements caused by E_{ur}^{ref} , E_{50}^{ref} and E_{oed}^{ref} produce corresponding fluctuations for different soils. However, the ranking of the parameters is almost invariant. According to all analysis, E_{ur}^{ref} is the parameter that has the largest influences the uncertainty in the MMC model. E_{oed}^{ref} is the least sensitive to horizontal displacement of diaphragm wall, that is, $E_{ur}^{ref} > E_{50}^{ref} > E_{oed}^{ref}$ (Fig. 5). By comparing the sensitivities of different soil layers with the same parameter, it can be seen that silty clay 4–1 is less sensitive to changes in parameters, which may be explained by that silty clay 4–1 has a higher moisture content.

The average sensitivities values of all soil layers of E_{ur}^{ref} , E_{50}^{ref} and E_{oed}^{ref} are 0.23 ± 0.07 , 0.11 ± 0.04 , 0.04 ± 0.01 , respectively. The sensitivities of E_{ur}^{ref} , E_{50}^{ref} and E_{oed}^{ref} are consistent with the sensitivities of three stiffness parameters in different soil layers, the difference between the measures of sensitivity for E_{ur}^{ref} and the rest of the parameters is significant.

3.3 Determination of E_{ur}^{ref} , E_{50}^{ref} and E_{oed}^{ref}

Horizontal displacement of diaphragm wall in different construction stages in different soil layers was compared

Fig. 5 Sensitivities of E_{ur}^{ref} , E_{50}^{ref} and E_{oed}^{ref} in different soil layers

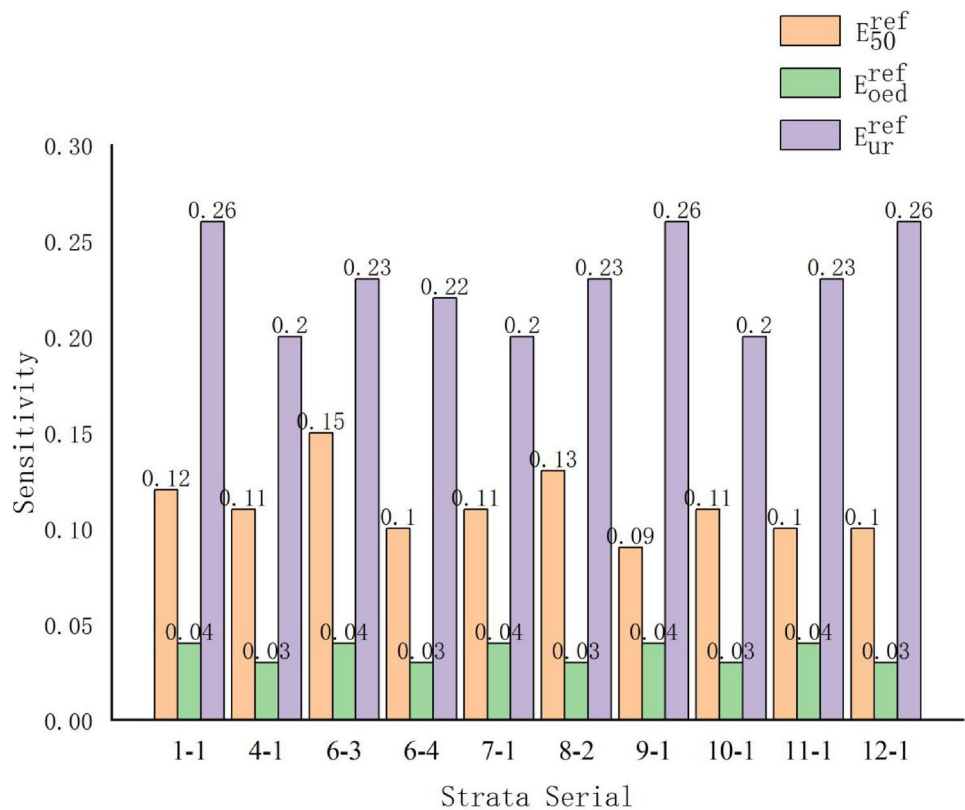


Fig. 6 Calculated and measured horizontal displacement curves of the diaphragm wall

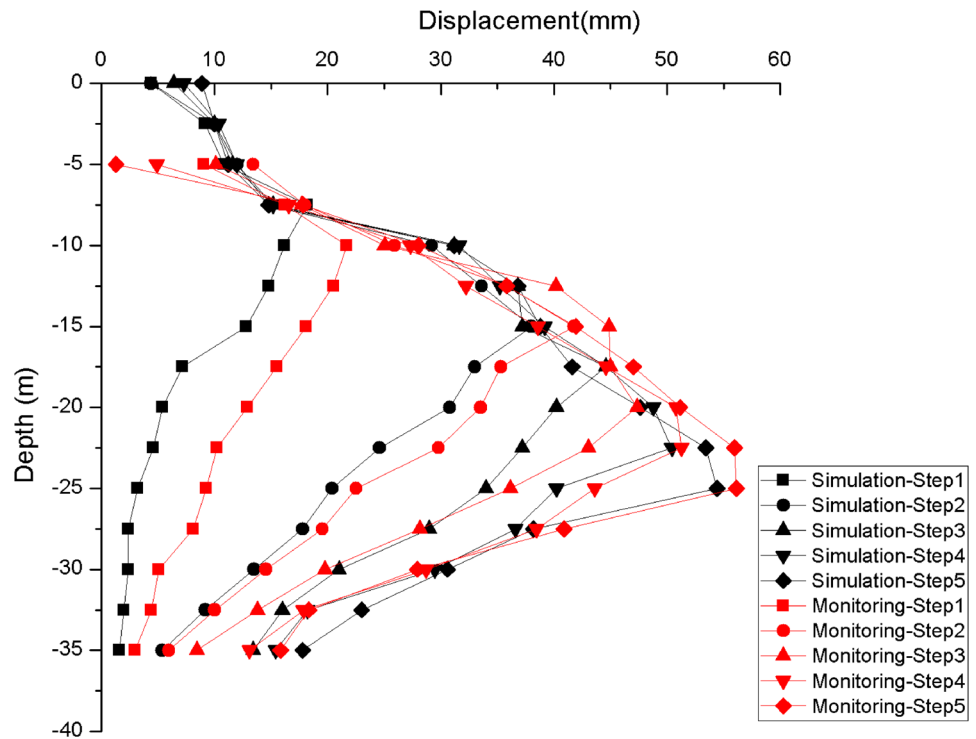


Table 3 Specific parameters of E_{ur}^{ref} , E_{50}^{ref} and E_{oed}^{ref}

Strata Serial	E_{50}^{ref}/MPa	E_{oed}^{ref}/MPa	E_{ur}^{ref}/MPa
1-1	3.08	4.62	9.24
4-1	4.58	6.88	13.75
6-3	7.91	11.87	23.74
6-4	4.27	6.41	12.82
7-1	4.21	6.31	12.62
8-2	8.61	12.91	25.82
9-1	4.49	6.73	13.46
10-1	5.01	7.51	15.02
11-1	5.29	7.93	15.86
12-1	5.54	8.30	16.61

Table 4 Regional experience stiffness parameter values

Region	E_{50}^{ref}	E_{oed}^{ref}	E_{ur}^{ref}
Beijing	E_0	$(0.5 \sim 1.0)E_{50}^{ref}$	$(2 \sim 4)E_{50}^{ref}$
Shanghai	$(0.9 \sim 1.0)E_0$	$(0.7 \sim 1.2)E_{50}^{ref}$	$(4 \sim 9)E_{50}^{ref}$
Tianjin	$(1.5 \sim 2.0)E_0$	$(1.0 \sim 1.5)E_{50}^{ref}$	$3 E_{50}^{ref}$

with the monitoring data, and the horizontal displacement diagram was drawn (Fig. 6). Figure 6 shows that the horizontal displacement of diaphragm wall is closest to the measured value for the five steps of foundation pit excavation. The parameter Settings that form the effect of

Table 5 E_{ur}^{ref} , E_{50}^{ref} and E_{oed}^{ref} explored by different researchers

References	Region
Wang et al.[41, 42]	Clay in Shanghai Sand
Pang et al.[43]	Granite residual soil in Shenzhen
Liu [44]	Soft soil in Tianjin
Duan [28]	Soft soil in Zhuhai
Zhou [45]	Clay Sand
Liu et al. [46]	Granite residual soil
Gebreselassie [47]	
Surarak [48]	Bangkok soft clay
Brinkgreve [49]	

Fig. 6 are shown in Table 3. Thus, it can be concluded that when $E_{ur}^{ref} = 3 E_{50}^{ref}$ and $E_{oed}^{ref} = 1.5 E_{50}^{ref}$, better simulation effect can be obtained. The values of E_{50}^{ref} , E_{oed}^{ref} and E_{ur}^{ref} required as input stiffness parameters of the MMC for each soil layer are summarized in Table 3, other parameters are selected according to Table 2.

4 Discussion

Soil stiffness parameters directly affect the deformation of foundation pit excavation. Through regional research results and analysis of correlation between stiffness parameters, the relationships between stiffness parameters in different regions are not the same. Regional experience stiffness parameter values for three regions are shown in Table 4. The results of soil stiffness parameters explored by different researchers in different regions are shown in Table 5.

To investigate the stiffness parameters of Tianjin water-rich soft soil relevant to simulation of deep excavation, a sensitivity analysis is conducted with a series of parameters taken by LH-OAT methods. Regardless of the same or different soil layers, E_{ur}^{ref} is most sensitive to horizontal displacement. The ratios ($E_{ur}^{ref}=3 E_{50}^{ref}$ and $E_{oed}^{ref}=1.5 E_{50}^{ref}$) determined in this study accord with common stiffness parameters and achieve good simulation results, which can provide reference for other foundation pit engineering simulation in Tianjin area.

E_s is the compression modulus of soil; E_0 is the elastic modulus of soil.

5 Conclusion

The MMC model is applied to simulate the foundation pit construction of the transfer station of the Tianjin city subway lines 11 (under construction) and 6 in this study. A sensitivity analysis by the LH-OAT method is conducted for the three parameters of the MMC model in 10 soil layers and the results of simulation are compared with the measured data, by taking the horizontal displacement of diaphragm wall as the evaluation target. It has been observed that the three parameters have a significant influence on the simulation of foundation pit excavation process.

For the horizontal displacement of diaphragm wall, the perturbation amplitude of 40% has been observed as the value results in minimal deformation while the perturbation amplitude of (-40%) represented the maximum deformation. The impact of E_{ur}^{ref} , E_{50}^{ref} and E_{oed}^{ref} can be ranked as follows: $E_{ur}^{ref} > E_{50}^{ref} > E_{oed}^{ref}$.

The sensitivity were normalized and sorted, and the sensitivity degree of each parameter to the control target was finally summarized. Comparing the sensitivities of the three parameters in different soil layers, it can be seen that E_{ur}^{ref} is the parameter that has the largest influence the uncertainty in the MMC model. E_{oed}^{ref} is the least sensitive to horizontal displacement of diaphragm wall.

On this basis, the stiffness ratio relationship suitable for foundation pit simulation in Tianjin water-rich soft soil area is obtained. the proportion relationship between stiffness parameters can be summarized as: $E_{ur}^{ref}=3 E_{50}^{ref}$ and $E_{oed}^{ref}=1.5 E_{50}^{ref}$.

In this paper, the influence of each parameter on the excavation process of foundation pit is determined by normalization. The subsequent construction can strictly monitor the sensitive parameters to reduce the deviation in the construction process as much as possible. The relationship between the stiffness parameters can provide reference for the deformation research of similar projects in the future.

Acknowledgements This research was funded by China Communications Construction Company (CCCC) First Highway Engineering Group Co. Ltd.(2021-KJYF-B-11).

Author Contributions Conceptualization, YZ and LY; methodology, LY and XH; validation, HL and HM; formal analysis, YY and XH; investigation, YY, XH and HL; resources, YZ and HM; data curation, HL and HM; writing—original draft preparation, XH; writing—review and editing, LY; supervision, YZ and HL; project administration, HL and HM funding acquisition, YZ All authors have read and agreed to the published version of the manuscript.

Funding This research was funded by China Communications Construction Company (CCCC) First Highway Engineering Group Co. Ltd. (2021-KJYF-B-11).

Data Availability Not applicable.

Declarations

Competing interests The authors declare no competing interests.

Conflict of interest The authors declare no conflict of interest.

Open Access This article is licensed under a Creative Commons Attribution 4.0 International License, which permits use, sharing, adaptation, distribution and reproduction in any medium or format, as long as you give appropriate credit to the original author(s) and the source, provide a link to the Creative Commons licence, and indicate if changes were made. The images or other third party material in this article are included in the article's Creative Commons licence, unless indicated otherwise in a credit line to the material. If material is not included in the article's Creative Commons licence and your intended use is not permitted by statutory regulation or exceeds the permitted use, you will need to obtain permission directly from the copyright holder. To view a copy of this licence, visit <http://creativecommons.org/licenses/by/4.0/>.

References

1. Meng Y (2016) Zhou S (2016) Discussion on the Engineering Properties of Soft Soil and Treatment

- Measures for Soft Foundation in Shenzhen. *Resources environment&Engineering* 30(03):450–453
2. Zhou CY, Mou CM (2004) Distribution and Microstructure Classification of Soft Clay in the Pearl River Delta. *Acta Sci Nat Univ Sunyatseni* 6:81–84
 3. Yang JX (1991) Distribution Patterns of Soft Soil Layers the Classification of Engineering Geology Layers in Tianjin Plain. *J Tianjin Univ* S2:126–131
 4. Fu BC, Huang Y, Li QS, Fu JQ (2000) Research of Cause and Classification of the Shallow Layer Soft Soil for Kunming Basin. *Journal of Kunming University of Science and Technology* 5:22–26
 5. Gan JJ, Wan S, Li JH, Tang C, Yang T, Luo ZQ (2019) Classification of lacustrine soft soils based on sedimentary environment and engineering characteristics: A case study of four typical soft soils in Poyang Lake Basin. *Geol Rev* 65(04):983–992
 6. Wang W J (2018) Study on the deformation of existing metro shield tunnel in soft soil area and the controlling techniques. Dissertation, Zhejiang University.
 7. Wang J, Zhang S, Teizer JJ, A i C, (2015) Geotechnical and Safety Protective Equipment Planning Using Range Point Cloud Data and Rule Checking in Building Information Modeling. *Autom Constr* 49:250–261
 8. Ji QX, Ge XS (2013) The Research on the Influence of the Forms of Foundation on the Behavior of Adjacent Excavation Based on Building Materials. *Adv Mat Res* 2621(788–788):606–610
 9. Wang YF, Zhou ZG, Gao HM (2011) Analysis on the Stress and Deformation of Deep Excavation Simulated by Multiplying ANSYS and ABAQUS. *Adv Mat Res* 1380(317–319):1729–1732
 10. Zhang ZG, Zhang MX, Wang WD (2011) Two-stage method for analyzing effects on adjacent metro tunnels due to foundation pit excavation. *Rock Soil Mech* 32(07):2085–2092
 11. Huang M, Liu XR, Zhang NY, Shen QW (2017) Calculation of foundation pit deformation caused by deep excavation considering influence of loading and unloading. *J Cent South Univ* 24(9):2164–2171
 12. Rouainia M, Elia G, Panayides S, Scott P (2017) Nonlinear Finite-Element Prediction of the Performance of a Deep Excavation in Boston Blue Clay. *J Geotech Geoenviron Eng* 143(5):
 13. Song G, Song EX (2014) Selection of Soil Constitutive Model for Numerical Simulation of Foundation Pit Excavation. *Engineering Mechanics* 31(05):86–94
 14. Wu B, Peng YY, Lan YB, Meng GW (2019) Response Analysis of Excavation of Deep Foundation Pit in Metro Station of Soft Soil. *IOP Conf Ser Earth Environ Sci* 330(2):022102–022102
 15. Xu ZH, Wang WD (2010) Selection of Soil Constitutive Model for Numerical Analysis of Deep Excavation in Close Proximity to Sensitive Properties. *Rock Soil Mech* 31(01):258–265
 16. Mohammad Z, Irfan AS (2021) Numerical Analysis of Himalayan Rock Tunnels under Static and Blast Loading. *Geotech Geol Eng* 39(7):1–21
 17. Mohammad Z, Md RS, Mohd MA (2021) Blast Resistant Analysis of Rock Tunnel Using Abaqus: Effect of Weathering. *Geotech Geol Eng* 40:809–832
 18. Brinkgreve, Ronald B J (2005) Selection of Soil Models and Parameters for Geotechnical Engineering Application. *Geofrontiers Congress*.
 19. Boonchai U, Andrew JW, Scott WS (2003) Undrained Stability of Braced Excavations in Clay. *Journal of Geotechnical and Geoenvironmental Engineering* 129(8):738–755
 20. Jonathan TH, Wu S-Y, Tung, (2020) Determination of Model Parameters for the Hardening Soil Model. *Transportation Infrastructure Geotechnology* 7(1):55–68
 21. Zoa Ambassa; J. C. Amba, (2020) Assessment of stiffness and strength parameters for the soft soil Model of clays of Cameroon. *Advances in Civil Engineering* 2020:1–16
 22. Zoa Ambassa; J. C. Amba, (2022) Towards an Advanced New Emerging Method of Determination of Mohr-Coulomb Parameters of Soils from at the Oedometer Test: Case Study-Lateritic Soils of Cameroon. *Math Probl Eng*. <https://doi.org/10.1155/2022/4222654>
 23. Calvello M (2002) Inverse analysis of supported excavations through Chicago glacial clays. Northwestern University.
 24. Finno RJ, Calvello M (2005) Supported excavations: observational method and inverse modeling. *Journal of Geotechnical and Geoenvironmental Engineering* 131(7):826–836
 25. Hashash YMA, Song H, Osouli A (2011) Threedimensional inverse analyses of a deep excavation in Chicago clays. *International Journal for Numerical and Analytical Method in Geomechanics* 35:1059–1075
 26. Xu X, Dai ZH (2017) Numerical implementation of a modified Mohr-Coulomb model and its application in slope stability analysis. *Journal of Modern Transportation* 25(01):40–51
 27. Schweiger HF (2008) The Role of Advanced Constitutive Models in Geotechnical Engineering. *Geomechanics and Tunneling* 1(5):336–344
 28. Duan S L (2020) Numerical Simulation Analysis of Reinforcement Effects of Skirt Border Improvement for a Soft Soil Foundation Pit in Zhuhai. Dissertation, South China University of Technology.
 29. Zheng T Y (2020) Research on Mechanical Properties of Deep Foundation Pit of Transfer Station in Soft Soil Based on HS Constitutive Model. Dissertation, Foshan University.
 30. Cudny M, Truty A (2020) Refinement of the Hardening Soil model within the small strain range. *Acta Geotech* 15:1–21
 31. Morris MD (1991) Factorial sampling plans for preliminary computational experiments. *Technometrics* 33(2):161–174
 32. Sobol'IM, (1993) Sensitivity estimates for nonlinear mathematical models. *Math Model Comput Exp* 1(4):407–414
 33. Saltelli A, Annoni P, Azzini I, Campolongo F, Ratto M, Tarantola S (2010) Variance based sensitivity analysis of model output. Design and estimator for the total sensitivity index. *Comput. Phys. Commun* 181(2): 259–270.
 34. Vandenbergh V, Griensven A, Bauwens W (2001) Sensitivity analysis and calibration of the parameters of ESWAT: application to the River Dender. *Water Sci Technol* 43(7):295–300
 35. Griensven A, Meixner T, Grunwald S, Bishop T, Diluzio A, Srinivasan R (2006) A global sensitivity analysis toolfor the parameters of multi-variable catchment models. *J Hydrol* 324(1–4):10–23
 36. Holvoet K, van Griensven A, Seuntjens P, Vanrolleghem PA (2005) Sensitivity analysis for hydrology and pesticide supply towards the river in SWAT. *Phys Chem Earth* 30(8–10):518–526
 37. Jung YW, Oh DS, Kim M, Park JW (2010) Calibration of LEACHN model using LH-OAT sensitivity analysis. *Nutr Cycl Agroecosyst* 87(2):261–275
 38. Qiao F, Bo JS, Qi WH, Wang L, Chang CY, Zhang ZP, Wang J (2020) Study on the dynamic characteristics of soft soil. *RSC Adv* 10(8):4630–4639
 39. Liu FR, Hu JF (2021) Analysis of genesis and physical and mechanical indexes of marine soft soil in Tianjin Binhai New Area. *Shanxi Architecture* 47(21):81–82
 40. Geotechnical Engineering Investigation Report of Heiniucheng Road Station, Tianjin Subway Line 11 (Detailed Investigation); Contract Technical Report; Tianjin Geological Survey Institute: Tianjin China 2018
 41. Wang WD, Wang HR, Xu ZH (2012) Experimental Study of Parameters of Hardening Soil Model for Numerical Analysis of Excavations of Foundation Pits. *Rock Soil Mech* 33(08):2283–2290
 42. Wang WD, Wang HR, Xu ZH (2013) Study of Parameters of HS-Small Model Used in Numerical Analysis of Excavations in Shanghai Area. *Rock Soil Mech* 34(06):1766–1774

43. Pang XC, Huang JJ, Su D, Xiao WH, Zhen ZT, Liu B (2018) Experimental Study on Parameters of the Hardening Soil Model for Undisturbed Granite Residual Soil in Shenzhen. *Rock Soil Mech* 39(11):4079–4085
44. Liu C (2008) Analysis of Deformation and Stress Due to Deep Excavation Considering Different Deformation and Strength Parameters of Soil and Space Effect of Excavation and Retaining Structure. Dissertation, Tianjin University.
45. Zhou E P (2010) Application of Hardening Soil Model with Small-strain Deformation Analysis for Foundation Pit. Dissertation, Harbin Institute of Technology.
46. Liu Z, Li ZC, Liu GN, Pang XC, Zhen ZT (2017) Study on Parameters Determination of Modified Mohr-Coulomb Model for Granite Residual Soil in Deep Foundation Pit Simulation Analysis. *Railw Eng* 03:89–92
47. Gebreselassie B (2003) Experimental, analytical and numerical investigations of excavations in normally consolidated soft soils. Dissertation. University of Kassel.
48. Surarak C, Likilersuang S, Wanatowski D, Balasubramaniam A, Oh E, Guan H (2012) Stiffness and strength parameters for hardening soil model and stiff Bangkok clays. *Soil and Foundation* 52(4):682–697
49. Brinkgreve R B J, Swolfs W M, Engin E, Waterman D, Chesaru A, Bonnier P G, Galavi V (2010) PLAXIS 2D 2010-Material models manual. Netherlands, pp 50–56.

Publisher's Note Springer Nature remains neutral with regard to jurisdictional claims in published maps and institutional affiliations.